EUROPEAN LABORATORY FOR PARTICLE PHYSICS

CERN-EP/98-118
20 July 1998

Study of D^0–$\bar{D}^0$ Mixing and D^0 Doubly Cabibbo-Suppressed Decays

The ALEPH Collaboration*

Abstract

Using a sample of four million hadronic Z events collected in ALEPH from 1991 to 1995, the decays $D^{*+} \to D^0\pi_s^+$, with D^0 decaying to $K^-\pi^+$ or to $K^+\pi^-$, are studied. The relative branching ratio $B(D^0 \to K^+\pi^-)/B(D^0 \to K^-\pi^+)$ is measured to be $(1.84 \pm 0.59(\text{stat.}) \pm 0.34(\text{syst.}))\%$. The two possible contributions to the $D^0 \to K^+\pi^-$ decay, doubly Cabibbo-suppressed decays and D^0–$\bar{D}^0$ mixing, are disentangled by measuring the proper-time distribution of the reconstructed D^0's. Assuming no interference between the two processes, the upper limit obtained on the mixing rate is 0.92% at 95% CL. The possible effect of interference between the two amplitudes is also assessed.

(Submitted to Physics Letters B)

*See the following pages for the list of authors.

The ALEPH Collaboration

R. Barate, D. Buskulic, D. Decamp, P. Ghez, C. Goy, J.-P. Lees, A. Lucotte, E. Merle, M.-N. Minard, J.-Y. Nief, B. Pietrzyk

Laboratoire de Physique des Particules (LAPP), IN^{2}P^3-CNRS, F-74019 Annecy-le-Vieux Cedex, France

R. Alemany, G. Boix, M.P. Casado, M. Chmeissani, J.M. Crespo, M. Delfino, E. Fernandez, M. Fernandez-Bosman, Ll. Garrido,[15] E. Graugès, A. Juste, M. Martinez, G. Merino, R. Miquel, Ll.M. Mir, I.C. Park, A. Pascual, I. Riu, F. Sanchez

Institut de Física d'Altes Energies, Universitat Autònoma de Barcelona, E-08193 Bellaterra (Barcelona), Spain[7]

A. Colaleo, D. Creanza, M. de Palma, G. Gelao, G. Iaselli, G. Maggi, M. Maggi, S. Nuzzo, A. Ranieri, G. Raso, F. Ruggieri, G. Selvaggi, L. Silvestris, P. Tempesta, A. Tricomi,[3] G. Zito

Dipartimento di Fisica, INFN Sezione di Bari, I-70126 Bari, Italy

X. Huang, J. Lin, Q. Ouyang, T. Wang, Y. Xie, R. Xu, S. Xue, J. Zhang, L. Zhang, W. Zhao

Institute of High-Energy Physics, Academia Sinica, Beijing, The People's Republic of China[8]

D. Abbaneo, U. Becker, P. Bright-Thomas,[24] D. Casper, M. Cattaneo, F. Cerutti, V. Ciulli, G. Dissertori, H. Drevermann, R.W. Forty, M. Frank, R. Hagelberg, A.W. Halley, J.B. Hansen, J. Harvey, P. Janot, B. Jost, I. Lehraus, P. Mato, A. Minten, L. Moneta,[21] A. Pacheco, F. Ranjard, L. Rolandi, D. Rousseau, D. Schlatter, M. Schmitt,[20] O. Schneider, W. Tejessy, F. Teubert, I.R. Tomalin, H. Wachsmuth

European Laboratory for Particle Physics (CERN), CH-1211 Geneva 23, Switzerland

Z. Ajaltouni, F. Badaud, G. Chazelle, O. Deschamps, A. Falvard, C. Ferdi, P. Gay, C. Guicheney, P. Henrard, J. Jousset, B. Michel, S. Monteil, J-C. Montret, D. Pallin, P. Perret, F. Podlyski, J. Proriol, P. Rosnet

Laboratoire de Physique Corpusculaire, Université Blaise Pascal, IN^{2}P^3-CNRS, Clermont-Ferrand, F-63177 Aubière, France

J.D. Hansen, J.R. Hansen, P.H. Hansen, B.S. Nilsson, B. Rensch, A. Wäänänen

Niels Bohr Institute, DK-2100 Copenhagen, Denmark[9]

G. Daskalakis, A. Kyriakis, C. Markou, E. Simopoulou, I. Siotis, A. Vayaki

Nuclear Research Center Demokritos (NRCD), GR-15310 Attiki, Greece

A. Blondel, G. Bonneaud, J.-C. Brient, P. Bourdon, A. Rougé, M. Rumpf, A. Valassi,[6] M. Verderi, H. Videau

Laboratoire de Physique Nucléaire et des Hautes Energies, Ecole Polytechnique, IN^{2}P^3-CNRS, F-91128 Palaiseau Cedex, France

E. Focardi, G. Parrini, K. Zachariadou

Dipartimento di Fisica, Università di Firenze, INFN Sezione di Firenze, I-50125 Firenze, Italy

M. Corden, C. Georgiopoulos, D.E. Jaffe

Supercomputer Computations Research Institute, Florida State University, Tallahassee, FL 32306-4052, USA [13,14]

A. Antonelli, G. Bencivenni, G. Bologna,[4] F. Bossi, P. Campana, G. Capon, V. Chiarella, G. Felici, P. Laurelli, G. Mannocchi,[5] F. Murtas, G.P. Murtas, L. Passalacqua, M. Pepe-Altarelli

Laboratori Nazionali dell'INFN (LNF-INFN), I-00044 Frascati, Italy

L. Curtis, J.G. Lynch, P. Negus, V. O'Shea, C. Raine, J.M. Scarr, K. Smith, P. Teixeira-Dias, A.S. Thompson, E. Thomson

Department of Physics and Astronomy, University of Glasgow, Glasgow G12 8QQ,United Kingdom[10]

O. Buchmüller, S. Dhamotharan, C. Geweniger, G. Graefe, P. Hanke, G. Hansper, V. Hepp, E.E. Kluge, A. Putzer, J. Sommer, K. Tittel, S. Werner, M. Wunsch

Institut für Hochenergiephysik, Universität Heidelberg, D-69120 Heidelberg, Germany[16]

R. Beuselinck, D.M. Binnie, W. Cameron, P.J. Dornan,[2] M. Girone, S. Goodsir, E.B. Martin, N. Marinelli, A. Moutoussi, J. Nash, J.K. Sedgbeer, P. Spagnolo, M.D. Williams

Department of Physics, Imperial College, London SW7 2BZ, United Kingdom[10]

V.M. Ghete, P. Girtler, E. Kneringer, D. Kuhn, G. Rudolph

Institut für Experimentalphysik, Universität Innsbruck, A-6020 Innsbruck, Austria[18]

A.P. Betteridge, C.K. Bowdery, P.G. Buck, P. Colrain, G. Crawford, A.J. Finch, F. Foster, G. Hughes, R.W.L. Jones, N.A. Robertson, M.I. Williams

Department of Physics, University of Lancaster, Lancaster LA1 4YB, United Kingdom[10]

I. Giehl, C. Hoffmann, K. Jakobs, K. Kleinknecht, G. Quast, B. Renk, E. Rohne, H.-G. Sander, P. van Gemmeren, C. Zeitnitz

Institut für Physik, Universität Mainz, D-55099 Mainz, Germany[16]

J.J. Aubert, C. Benchouk, A. Bonissent, G. Bujosa, J. Carr,[2] P. Coyle, F. Etienne, O. Leroy, F. Motsch, P. Payre, M. Talby, A. Sadouki, M. Thulasidas, K. Trabelsi

Centre de Physique des Particules, Faculté des Sciences de Luminy, IN^{2}P^3-CNRS, F-13288 Marseille, France

M. Aleppo, M. Antonelli, F. Ragusa

Dipartimento di Fisica, Università di Milano e INFN Sezione di Milano, I-20133 Milano, Italy

R. Berlich, V. Büscher, G. Cowan, H. Dietl, G. Ganis, G. Lütjens, C. Mannert, W. Männer, H.-G. Moser, S. Schael, R. Settles, H. Seywerd, H. Stenzel, W. Wiedenmann, G. Wolf

Max-Planck-Institut für Physik, Werner-Heisenberg-Institut, D-80805 München, Germany[16]

J. Boucrot, O. Callot, S. Chen, A. Cordier, M. Davier, L. Duflot, J.-F. Grivaz, Ph. Heusse, A. Höcker, A. Jacholkowska, D.W. Kim,[12] F. Le Diberder, J. Lefrançois, A.-M. Lutz, M.-H. Schune, E. Tournefier, J.-J. Veillet, I. Videau, D. Zerwas

Laboratoire de l'Accélérateur Linéaire, Université de Paris-Sud, IN^{2}P^3-CNRS, F-91898 Orsay Cedex, France

P. Azzurri, G. Bagliesi,[2] G. Batignani, S. Bettarini, T. Boccali, C. Bozzi, G. Calderini, M. Carpinelli, M.A. Ciocci, R. Dell'Orso, R. Fantechi, I. Ferrante, L. Foà,[1] F. Forti, A. Giassi, M.A. Giorgi, A. Gregorio, F. Ligabue, A. Lusiani, P.S. Marrocchesi, A. Messineo, F. Palla, G. Rizzo, G. Sanguinetti, A. Sciabà, G. Sguazzoni, R. Tenchini, G. Tonelli,[19] C. Vannini, A. Venturi, P.G. Verdini

Dipartimento di Fisica dell'Università, INFN Sezione di Pisa, e Scuola Normale Superiore, I-56010 Pisa, Italy

G.A. Blair, L.M. Bryant, J.T. Chambers, M.G. Green, T. Medcalf, P. Perrodo, J.A. Strong, J.H. von Wimmersperg-Toeller

Department of Physics, Royal Holloway & Bedford New College, University of London, Surrey TW20 OEX, United Kingdom[10]

D.R. Botterill, R.W. Clifft, T.R. Edgecock, P.R. Norton, J.C. Thompson, A.E. Wright

Particle Physics Dept., Rutherford Appleton Laboratory, Chilton, Didcot, Oxon OX11 OQX, United Kingdom[10]

B. Bloch-Devaux, P. Colas, S. Emery, W. Kozanecki, E. Lançon,[2] M.-C. Lemaire, E. Locci, P. Perez, J. Rander, J.-F. Renardy, A. Roussarie, J.-P. Schuller, J. Schwindling, A. Trabelsi, B. Vallage

CEA, DAPNIA/Service de Physique des Particules, CE-Saclay, F-91191 Gif-sur-Yvette Cedex, France[17]

S.N. Black, J.H. Dann, R.P. Johnson, H.Y. Kim, N. Konstantinidis, A.M. Litke, M.A. McNeil, G. Taylor

Institute for Particle Physics, University of California at Santa Cruz, Santa Cruz, CA 95064, USA[22]

C.N. Booth, S. Cartwright, F. Combley, M.S. Kelly, M. Lehto, L.F. Thompson

Department of Physics, University of Sheffield, Sheffield S3 7RH, United Kingdom[10]

K. Affholderbach, A. Böhrer, S. Brandt, C. Grupen, P. Saraiva, L. Smolik, F. Stephan

Fachbereich Physik, Universität Siegen, D-57068 Siegen, Germany[16]

G. Giannini, B. Gobbo, G. Musolino

Dipartimento di Fisica, Università di Trieste e INFN Sezione di Trieste, I-34127 Trieste, Italy

J. Rothberg, S. Wasserbaech

Experimental Elementary Particle Physics, University of Washington, WA 98195 Seattle, U.S.A.

S.R. Armstrong, E. Charles, P. Elmer, D.P.S. Ferguson, Y. Gao, S. González, T.C. Greening, O.J. Hayes, H. Hu, S. Jin, P.A. McNamara III, J.M. Nachtman,[23] J. Nielsen, W. Orejudos, Y.B. Pan, Y. Saadi, I.J. Scott, J. Walsh, Sau Lan Wu, X. Wu, G. Zobernig

Department of Physics, University of Wisconsin, Madison, WI 53706, USA[11]

[1]Now at CERN, 1211 Geneva 23, Switzerland.
[2]Also at CERN, 1211 Geneva 23, Switzerland.
[3]Also at Dipartimento di Fisica, INFN, Sezione di Catania, Catania, Italy.
[4]Also Istituto di Fisica Generale, Università di Torino, Torino, Italy.
[5]Also Istituto di Cosmo-Geofisica del C.N.R., Torino, Italy.
[6]Supported by the Commission of the European Communities, contract ERBCHBICT941234.
[7]Supported by CICYT, Spain.
[8]Supported by the National Science Foundation of China.
[9]Supported by the Danish Natural Science Research Council.
[10]Supported by the UK Particle Physics and Astronomy Research Council.
[11]Supported by the US Department of Energy, grant DE-FG0295-ER40896.
[12]Permanent address: Kangnung National University, Kangnung, Korea.
[13]Supported by the US Department of Energy, contract DE-FG05-92ER40742.
[14]Supported by the US Department of Energy, contract DE-FC05-85ER250000.
[15]Permanent address: Universitat de Barcelona, 08208 Barcelona, Spain.
[16]Supported by the Bundesministerium für Bildung, Wissenschaft, Forschung und Technologie, Germany.
[17]Supported by the Direction des Sciences de la Matière, C.E.A.
[18]Supported by Fonds zur Förderung der wissenschaftlichen Forschung, Austria.
[19]Also at Istituto di Matematica e Fisica, Università di Sassari, Sassari, Italy.
[20]Now at Harvard University, Cambridge, MA 02138, U.S.A.
[21]Now at University of Geneva, 1211 Geneva 4, Switzerland.
[22]Supported by the US Department of Energy, grant DE-FG03-92ER40689.
[23]Now at University of California at Los Angeles (UCLA), Los Angeles, CA 90024, U.S.A.
[24]Now at School of Physics and Astronomy, Birmingham B15 2TT, U.K.

1 Introduction

The D^0 can produce a $K^+\pi^-$ system either via a doubly Cabibbo-suppressed decay (DCSD) or via the oscillation of the D^0 into a $\bar{D}^0$ followed by the Cabibbo-favoured decay $\bar{D}^0 \to K^+\pi^-$. The rate of DCSD processes $D^0 \to K^+\pi^-$ is expected to be of the order of $2\tan^4\theta_C \sim 0.6\%$ [1], where θ_C is the Cabibbo angle. Within the framework of the Standard Model the D^0–$\bar{D}^0$ mixing rate $R_{\rm mix}$ is expected to be well below present experimental bounds [2, 3]. While short distance effects from box diagrams are known to give a small contribution ($R_{\rm mix} \sim 10^{-10}$) [4], long distance effects from second-order weak interactions with mesonic intermediate states may give a much larger contribution but are subject to large theoretical uncertainties ($R_{\rm mix} \sim 10^{-7} - 10^{-3}$) [5].

There are many extensions of the Standard Model which allow a D^0–$\bar{D}^0$ mixing rate significantly larger than the Standard Model prediction, for example models with leptoquarks, with two-Higgs-doublet, with fourth quark generation and supersymmetric models with alignment [6, 7]. Experimental evidence for mixing within the current experimental sensitivity would therefore be an indication of new physics.

The search for DCSD or mixing necessitates the identification of a change in the charm quantum number between production and decay of the D^0. The method presented here consists of reconstructing the $D^{*+} \to D^0\pi_s^+$ decay where the charge of the slow pion indicates whether a D^0 or a $\bar{D}^0$ is produced. The charge of the kaon in the subsequent $D^0 \to K\pi$ decay tags the charm flavour at decay. The relative contributions of the DCSD process and the D^0–$\bar{D}^0$ mixing are assessed by studying the proper-time distribution of the reconstructed D^0's.

2 ALEPH Detector and Data Selection

This analysis uses data collected in the vicinity of the Z peak from 1991 to 1995 with the ALEPH detector at the LEP electron-positron storage ring. The data sample consists of about four million hadronic Z decays that satisfy the criteria of Ref. [8].

A detailed description of the design and performance of the apparatus can be found in Refs. [9, 10], and only a brief summary of the features relevant to this study is given here. A double-sided silicon vertex detector (VDET), surrounding the beam pipe, is installed close to the interaction region. The single-hit resolution for the $r\phi$ and z projections is 12 μm. Outside the vertex detector are an eight-layer drift chamber, the inner tracking chamber (ITC), and a large time projection chamber (TPC). These three detectors form the tracking system, which is immersed in a 1.5 T axial magnetic field. Using the VDET, ITC and TPC coordinates the particle momentum transverse to the beam axis is measured with a resolution of $\delta p_{\rm T}/p_{\rm T} = 6 \times 10^{-4} p_{\rm T} \oplus 5 \times 10^{-3}$ ($p_{\rm T}$ in GeV/c).

The TPC also provides up to 338 measurements of the specific ionization of a charged particle. In the following, the dE/dx information is considered as available if more than 50 samples are present. Particle identification is based on the dE/dx estimators χ_π ($\chi_{\rm K}$), defined as the difference between the measured and expected ionization expressed in terms of standard deviations for the π (K) mass hypothesis. For charged tracks having momentum above 2 GeV/c a pion/kaon separation of 2σ is achieved.

3 Measurement of $B(\mathrm{D^0} \to \mathrm{K^+\pi^-})/B(\mathrm{D^0} \to \mathrm{K^-\pi^+})$

Starting from the sample of hadronic Z decays the $\mathrm{D}^{*\pm}$ are reconstructed as follows. Each pair of oppositely-charged tracks is considered with the two mass assignments $\mathrm{K}^-\pi^+$ and $\pi^-\mathrm{K}^+$ and those with $\mid M(\mathrm{K}\pi) - M_{\mathrm{D}^0} \mid < 30$ MeV/c^2 are retained. If both hypotheses satisfy the mass cut the event is rejected. In addition, the measured mean ionization of each track is required to be closer, in terms of number of standard deviations, to the expectation for the assumed mass hypothesis than for the alternative hypothesis. The decay angle θ^*_{K} of the kaon in the D^0 rest frame is required to satisfy $\mid \cos\theta^*_{\mathrm{K}} \mid \leq 0.8$. Only combinations in which the two tracks form a common vertex and each track has at least one VDET hit are kept.

To build the $\mathrm{D}^{*\pm}$ candidate the surviving track pairs are combined with an extra charged track, the "soft pion" (π_s), of low momentum, typically less than 4 GeV/c [11] (the limits on momentum are fixed by kinematics and resolution effects). In order to reduce the combinatorial background, the energy of the $\mathrm{D}^{*\pm}$ candidate is required to be greater than half the beam energy.

The Cabibbo-favoured decays of the D^0 and $\bar{\mathrm{D}}^0$ are contained in the sample for which the two pions have the same sign (right-sign sample), while the DCSDs and mixing candidates are contained in the sample for which the two pions have opposite sign (wrong-sign sample). The $\Delta M = M_{\pi_s \mathrm{D}^0} - M_{\mathrm{D}^0}$ distributions of the right-sign and wrong-sign samples are shown in Fig. 1 together with the estimated combinatorial background. The shape of this combinatorial background is assumed to be the same as that obtained from events in the sideband region of the D^0 invariant mass distribution above 2.1 GeV/c^2, and is normalised to the number of candidates having $\Delta M > 160$ MeV/c^2.

Within a ΔM mass window from 143.5 MeV/c^2 to 147.5 MeV/c^2 the numbers of events in the right-sign and the wrong-sign samples after the combinatorial background is subtracted are

$$N_{\mathrm{RS}} = 1038.8 \pm 32.5(\mathrm{stat.}) \pm 4.3(\mathrm{syst.}) \ ,$$

$$N_{\mathrm{WS}} = 21.3 \pm 6.1(\mathrm{stat.}) \pm 3.4(\mathrm{syst.}) \ ,$$

respectively. The systematic error is due to the limited statistics used to determine the combinatorial background.

Monte Carlo studies show that, although the physics background contamination in the right-sign sample is negligible, a small contribution from physics backgrounds must be subtracted from the wrong-sign sample. Four decay modes are found to contribute, namely: $\mathrm{D}^0 \to \mathrm{K}^-\pi^+(\pi^0)$, $\mathrm{D}^0 \to \pi^-\mu^+\nu_\mu$, $\mathrm{D}^0 \to \pi^+\pi^-\pi^0$ and $\mathrm{D}^0 \to \mathrm{K}^-\mathrm{K}^+$. They contribute because of misidentification of one or both tracks or because of missing neutrinos or π^0s.

To demonstrate that the peak appearing in Fig. 1b is not related to combinatorial background, events are selected in the ΔM mass window and the cut on $M(\mathrm{K}\pi)$ for the wrong-sign sample is not applied. The resulting $M(\mathrm{K}\pi)$ distribution is shown in Fig. 2. A narrow peak at the nominal D^0 mass ($M_{\mathrm{D}^0} = 1864.5$ GeV/c^2) is present. The peak on the left, due to $\mathrm{D}^0 \to \mathrm{K}^-\mathrm{K}^+$ decays, is outside the D^0 mass window.

Rather than relying on the Monte Carlo estimates for the physics background subtraction, the data are used to estimate the contribution of the dominant $\mathrm{D}^0 \to \mathrm{K}^-\pi^+(\pi^0)$ physics background to the wrong-sign sample. This is achieved by repeating

the selection, with the dE/dx requirement reversed, i.e. the ionization of the kaon (pion) candidate has to be closer to the expectation for a pion (kaon). This sample is hereafter called $\overline{dE/dx}$. In this sample the $D^0 \to K^-\pi^+(\pi^0)$ contribution is strongly enhanced while the DCSD/mixing signal is suppressed by the same factor. The contributions from the other decay channels remain the same, since the cut is symmetric when the mass hypotheses are reversed.

According to Monte Carlo studies, the $\overline{dE/dx}$ sample also contains some small additional physics backgrounds, from semileptonic D^0 decay channels, and these must also be taken into account. Table 1 shows the number of expected physics background candidates for the dE/dx and $\overline{dE/dx}$ samples, calculated from the Monte Carlo efficiencies and assuming the Particle Data Group [12] branching ratios.

Channel	dE/dx	$\overline{dE/dx}$
$D^0 \to K^-\pi^+(\pi^0)$	1.56 ± 1.08	26.48 ± 4.16
$D^0 \to \pi^-\pi^+\pi^0$	0.36 ± 0.36	0.36 ± 0.36
$D^0 \to \pi^-\mu^+\nu_\mu$	0.16 ± 0.16	0.16 ± 0.16
$D^0 \to K^-K^+$	0.12 ± 0.12	0.12 ± 0.12
$D^0 \to K^-e^+\nu_e$	–	3.16 ± 1.20
$D^0 \to K^-\mu^+\nu_\mu$	–	0.84 ± 0.64

Table 1: Physics background estimated from the Monte Carlo with the standard and reversed dE/dx cuts.

The expected contributions after the subtraction of the combinatorial background to the number of candidates of the wrong-sign sample, $N_{\rm WS}$, and the number of candidates of the $\overline{dE/dx}$ sample, $N_{\rm WS}^{\overline{dE/dx}}$, can be written as

$$N_{\rm WS} = N_{D^0\to K^+\pi^-} + N_{K\pi(\pi^0)} + N_{\rm symm} \quad (1)$$

$$N_{\rm WS}^{\overline{dE/dx}} = \frac{1}{r}N_{D^0\to K^+\pi^-} + rN_{K\pi(\pi^0)} + N_{\rm symm} + N_{\rm other} \quad (2)$$

where the various quantities are explicited hereafter.

- $\boldsymbol{N_{D^0\to K^+\pi^-}}$ is the unknown number of events attributed to the DCSD/mixing signal in the wrong-sign sample.
- $\boldsymbol{N_{K\pi(\pi^0)}}$ is the unknown number of events attributed to the dominant $D^0 \to K^-\pi^+(\pi^0)$ physics background in the wrong sign sample.
- $\boldsymbol{r}$ is the known enhancement factor for the $D^0 \to K^-\pi^+(\pi^0)$ contribution obtained when the dE/dx cut is reversed. This is measured in the data to be $r = 46.1 \pm 11.8$, by applying the reversed dE/dx cuts to the right-sign sample and noting the reduction in the size of the peak from the Cabibbo-favoured D^0 decay.

- $\boldsymbol{N_{\rm symm}}$ is the estimate of the sum of the backgrounds which are symmetric upon reversal of the dE/dx cut, i.e. the $\rm D^0 \to \pi^-\pi^+\pi^0$, $\rm D^0 \to \pi^-\mu^+\nu_\mu$ and $\rm D^0 \to K^-K^+$ backgrounds. $N_{\rm symm}$ is assumed to be $rN_{\rm K\pi(\pi^0)} \cdot f_{\rm symm}$, where $f_{\rm symm}$ is the fraction of symmetric events with respect the number of $\rm K\pi(\pi^0)$ events in the Monte Carlo $\overline{dE/dx}$ sample. The error on this number is taken to be 100% to take into account the differences, compatible with statistical fluctuations, found both for the dE/dx and $\overline{dE/dx}$ samples in Monte Carlo.

- $\boldsymbol{N_{\rm other}}$ is the additional backgrounds expected in the $\overline{dE/dx}$ sample coming from $\rm D^0 \to K^-e^+\nu_e$ and $\rm D^0 \to K^-\mu^+\nu_\mu$ decays. It is assumed to be $rN_{\rm K\pi(\pi^0)} \cdot f_{\rm other}$, where $f_{\rm other}$ is also taken from the Monte Carlo estimate. The uncertainties are due to the limited statistics and to the errors on the branching ratios.

Using the values $N_{\rm WS} = 21.3 \pm 6.1({\rm stat.}) \pm 3.4({\rm syst.})$, $N_{\rm WS}^{\overline{dE/dx}} = 56.4 \pm 8.1({\rm stat.}) \pm 2.3({\rm syst.})$ measured in the data, equations (1) and (2) yield

$$N_{\rm K\pi(\pi^0)} = 1.03 \pm 0.15({\rm stat.}) \pm 0.27({\rm syst.}) \ ,$$

$$N_{\rm D^0 \to K^+\pi^-} = 19.1 \pm 6.1({\rm stat.}) \pm 3.5({\rm syst.}) \ .$$

The total physical background ($N_{\rm K\pi(\pi^0)} + N_{\rm symm}$) is 2.2 ± 1.0 and is consistent with the Monte Carlo expectation of 2.2 ± 1.2 from Table 1. The systematic uncertainties for $N_{\rm D^0 \to K^+\pi^-}$ are listed in Table 2 and are derived by varying the following quantities by one standard deviation: (i) the systematic uncertainty on $N_{\rm WS}$ due to the combinatorial background subtraction, (ii) the statistical and systematic uncertainties on the $N_{\rm WS}^{\overline{dE/dx}}$ sample, (iii) the statistical uncertainty on r and finally (iv) the uncertainties on the physics background processes as discussed previously.

Dividing $N_{\rm D^0 \to K^+\pi^-}$ by the number of signal events in the right-sign sample ($N_{\rm RS}$) yields a relative branching ratio of

$$B(\rm D^0 \to K^+\pi^-)/B(D^0 \to K^-\pi^+) = (1.84 \pm 0.59({\rm stat.}) \pm 0.34({\rm syst.}))\% \ .$$

Source	Systematics
Syst. error on $N_{\rm WS}$	± 3.4
Stat. error on $N_{\rm WS}^{\overline{dE/dx}}$	± 0.3
Syst. error on $N_{\rm WS}^{\overline{dE/dx}}$	± 0.1
r = effic.(dE/dx)/effic.$(\overline{dE/dx})$	± 0.3
Fractions of physics background	± 0.9
Total	± 3.5

Table 2: Systematic uncertainties for the measurement of the number of $\rm D^0 \to K^+\pi^-$ decays.

4 Proper Time Distribution

Assuming small mixing and neglecting CP-violating terms, the time evolution for the signal in the wrong sign sample is expected to have the following form [13]

$$N_{\mathrm{D}^0\to\mathrm{K}^+\pi^-}(t) \propto \left[R_{\mathrm{DCSD}} + \sqrt{2R_{\mathrm{mix}}R_{\mathrm{DCSD}}}t/\tau\cos\phi + R_{\mathrm{mix}}\frac{1}{2}(t/\tau)^2\right] e^{-t/\tau} \ , \qquad (3)$$

where R_{DCSD} is the ratio of doubly Cabibbo-suppressed over Cabibbo-favoured decays, R_{mix} is the ratio $B(\mathrm{D}^0 \to \bar{\mathrm{D}}^0 \to \mathrm{K}^+\pi^-)/B(\mathrm{D}^0 \to \mathrm{K}^-\pi^+)$ and $\cos\phi$ is the phase angle parametrizing the interference between the two processes. The first term, due to the DCSD decay, has the conventional exponential proper time dependence with a decay constant given by the D^0 lifetime. The third term is the contribution from the mixed events and peaks at $t/\tau = 2$. The second term accounts for possible interference between both processes. The significant differences in the structure of the proper time distributions for the DCSD and the mixing signals allow their respective contributions to be estimated.

The proper time $t = \ell\frac{M}{p}$ of a D^0 candidate is calculated from the decay length ℓ, defined as the distance between the primary vertex and the D^0 decay vertex projected along the direction of flight of the D^0, and the reconstructed momentum p and mass M of the candidate. The average resolution on the proper time is ≈ 0.1 ps and is dominated by the uncertainty on the position of the D^0 vertex.

The distributions of proper time in the signal region for the wrong-sign sample observed in the data is shown in Figure 3a. The result of a binned maximum likelihood fit is also shown. The following contributions are included in the probability density of the likelihood function:

- A direct $\mathrm{c\bar{c}} \to \mathrm{D}^0\mathrm{X}$ component, which has the proper time dependence given by Eq. 3 convoluted with the detector resolution. The number of events attributed to the DCSD signal and the mixing signal are left free in the fit. Various assumptions for the phase of the interference term are investigated.

  The fraction of the signal which is attributed to $\mathrm{c\bar{c}} \to \mathrm{D}^0\mathrm{X}$, (rather than the $\mathrm{b\bar{b}} \to \mathrm{c\bar{c}} \to \mathrm{D}^0\mathrm{X}$ discussed next) is $f_{\mathrm{c}}^{\mathrm{K}\pi} = (77.0 \pm 2.7(\mathrm{stat.}) \pm 0.5(\mathrm{syst.}))\%$. It is extracted from the data using a likelihood fit to the proper time dependence of the right-sign sample. This fit is essentially the same as the fit to the wrong-sign sample except that proper time dependence of the Cabibbo-favoured events is assumed to be exponential, as expected for small mixing, and the contribution accounting for the physics background is not necessary. The result of this fit is shown in Figure 3b.

- An indirect $\mathrm{b\bar{b}} \to \mathrm{c\bar{c}} \to \mathrm{D}^0\mathrm{X}$ component, which has the same proper time dependence as the direct component of the signal, but modified to take into account the effect of the additional flight distance of the B meson. The exact shape for this component is taken from Monte Carlo after appropriate reweighting for the world average B hadron and D^0 lifetimes [12].

- A physics background contribution for which the proper time dependence is assumed to be exponential with a decay constant given by the D^0 lifetime. The number of events attributed to this process is 2.2 ± 1.0, as determined in section 3.

Source of uncertainty	unconstrained fit		constrained fit
	$N_{\rm mix}$	$N_{\rm DCSD}$	$N_{\rm DCSD}$
Resolution	< 0.1	± 0.1	< 0.1
D^0 lifetime	< 0.1	< 0.1	< 0.1
Comb. back. distribution	± 0.7	± 1.4	± 1.1
Comb. back. rate	± 0.8	± 3.6	± 2.8
Charm fraction	± 0.4	± 0.3	± 0.1
Phys. back. rate		± 1.0	± 1.0
Total	± 1.1	± 4.0	± 3.2

Table 3: List of systematic uncertainties contributing to $N_{\rm DCSD}$ and $N_{\rm mix}$ for the case of no interference. The constrained fit results are obtained with $N_{\rm mix}$ constrained to be non-negative.

- A combinatorial background contribution, for which the proper time dependence is measured in the data from the sideband regions of the ΔM plot. The number of events attributed to this process is 15.7 ± 3.4 events.

For all the above contributions, except the combinatorial background, an additional proper time smearing of $(29 \pm 12)\%$ is applied to take into account that the proper time resolution measured in the data is slightly worse than that predicted by the Monte Carlo. This Monte Carlo/data comparison is performed by selecting candidates from the side band of the Kπ mass distribution both in Monte Carlo and data and comparing the width of a Gaussian fit to the negative proper time distribution of these events. To enhance the fraction of tracks in this sample coming from the interaction point the contamination from $c\bar{c}$ and $b\bar{b}$ events is suppressed by applying to the opposite hemisphere the lifetime tag veto described in Ref. [14].

Setting the interference term to zero ($\cos\phi = 0$), the result of the fit to the proper time distribution of the wrong-sign sample is

$$\begin{aligned} N_{\rm DCSD} &= 20.8^{+8.4}_{-7.4}({\rm stat.}) \pm 4.0({\rm syst.}) \ , \\ N_{\rm mix} &= -2.0 \pm 4.4({\rm stat.}) \pm 1.1({\rm syst.}) \ . \end{aligned}$$

The fitted value for $N_{\rm mix}$ is outside the physical region, thus no mixing is observed. Table 3 summarises all the sources of systematic uncertainty considered. They are computed by varying by one standard deviation on the fit the additional proper time smearing, the D^0 lifetime, the charm fraction and the combinatorial and physical background rates. The systematic uncertainties due to the combinatorial background proper time shape is evaluated by repeating the fit many times with a new combinatorial background shape, obtained by randomly varying the contents of each proper time bin according to a Poisson distribution.

Figure 4 shows the time dependence of the ratio of wrong-sign over the right-sign candidates after the background subtraction.

If $N_{\rm mix}$ is constrained to be non-negative, the result is

$$N_{\rm DCSD} = 18.4^{+6.2}_{-5.8}({\rm stat.}) \pm 3.2({\rm syst.}) \ ,$$

$$N_{\rm mix} = 0^{+3.0}({\rm stat.})^{+1.4}({\rm syst.})$$

which translates to

$$R_{\rm DCSD} = \left(1.77^{+0.60}_{-0.56}({\rm stat.}) \pm 0.31({\rm syst.})\right)\% \ .$$

In this case the systematic uncertainty on $N_{\rm mix}$ is obtained by adding to the likelihood used to fit the data, additional Gaussian terms for the extra smearing on the time resolution, the $\rm D^0$ lifetime, the charm fraction and the physical background rate, and Poissonian terms for the combinatorial background rate and shape. Figure 5 shows the resulting likelihood as a function of the assumed mixed fraction. By integrating the resulting likelihood over the allowed region an upper limit of $N_{\rm mix} < 9.6$ at 95% confidence level is obtained, corresponding to

$$R_{\rm mix} < 0.92\% \ \text{ at 95\% CL.}$$

The effect of interference has been studied by fitting the data with fully constructive ($\cos\phi = +1$) and fully destructive interference ($\cos\phi = -1$); the respective upper limits are $R_{\rm mix} < 0.96\%$ at 95% CL and $R_{\rm mix} < 3.6\%$ at 95% CL. For the case $\cos\phi = -1$ $N_{\rm mix} = 14.8^{+12.1}_{-13.3}({\rm stat.}) \pm 3.3({\rm syst.})$.

5 Conclusion

The $\rm D^0 \to K^+\pi^-$ decay is studied to determine the branching ratio $B(\rm D^0 \to K^+\pi^-)/B(D^0 \to K^-\pi^+)$. The method consists in reconstructing the $\rm D^{*+} \to D^0\pi_s^+$ decay where the $\rm D^0$ can subsequently decay to $\rm K^+\pi^-$ or $\rm K^-\pi^+$. The numbers of reconstructed decays observed after background subtraction give

$$B(\rm D^0 \to K^+\pi^-)/B(D^0 \to K^-\pi^+) = (1.84 \pm 0.59({\rm stat.}) \pm 0.34({\rm syst.}))\% \ .$$

This is 1.4 standard deviations from the CLEO [15] measurement $B(\rm D^0 \to K^+\pi^-)/B(D^0 \to K^-\pi^+) = (0.77 \pm 0.25({\rm stat.}) \pm 0.25({\rm syst.}))\%$.

In order to distinguish the two possible contributing processes, the fraction of doubly Cabibbo-suppressed decays $R_{\rm DCSD}$ and $\rm D^0$–$\bar{\rm D}^0$ mixing rate $R_{\rm mix}$, the proper time distribution is analysed, yielding

$$R_{\rm DCSD} = \left(1.77^{+0.60}_{-0.56}({\rm stat.}) \pm 0.31({\rm syst.})\right)\% \ ,$$

$$R_{\rm mix} < 0.92\% \ \text{ at 95\% CL} \ ,$$

assuming no interference between the two processes. The fit is improved if destructive interference is allowed.

This can be compared with the results obtained by the E691 Collaboration [16]: $R_{\rm DCSD} < 1.5\%$ at 90% CL based on the number of observed events $N_{\rm DCSD} = 1.8 \pm 13.2$, and $R_{\rm mix} < 0.5\%$ at 90% CL. The E791 collab. [17] finds $R_{\rm DCSD} = \left(0.68^{+0.34}_{-0.33}({\rm stat.}) \pm 0.07({\rm syst.})\right)\%$, for $R_{\rm mix} = 0$, in agreement within 1.5 standard deviations with our result, and sets a limit $R_{\rm mix} < 0.85\%$ at 90% CL allowing CP violation in the interference term.

Acknowledgement

We wish to congratulate our colleagues in the CERN accelerator divisions for successfully operating the LEP storage ring. We are grateful to the engineers and technicians in all our institutions for their contribution towards ALEPH's success. Those of us from non-member countries thank CERN for its hospitality.

References

[1] I. Bigi and A.I. Sanda, Phys. Lett. B 171 (1986) 320;
L.L. Chau and H.Y. Cheng, Phys. Lett. B 333 (1994) 514;
I. Hincliffe and T.A. Kaeding, Phys. Rev. D54 (1996) 914;
F. Buccella, M. Lusignoli and A. Pugliese, Phys. Lett. B 379 (1996) 249.

[2] H. Georgi, Phys. Lett. B 297 (1992) 353;
T. Ohl, G. Ricciardi and E.H. Simmons, Nucl. Phys. B 403, (1993) 603.

[3] G. Burdman, *Charm mixing and CP violation in the Standard Model*, Proceedings of the Charm 2000 Workshop, FERMILAB-Conf-94/190, Fermilab, June 7-9, 1994.

[4] M.K. Gaillard and B.W. Lee, Phys. Rev. D 10 (1974) 897;
A. Datta, Phys. Lett. B 154, (1985) 287;
A. Datta and M. Khambkhar, Z. Phys. C 27 (1985) 515;
A.A. Petrov, Phys. Rev. D 56 (1997) 1685.

[5] L. Wolfenstein, Phys. Lett. B 164 (1985) 170;
J. Donoghue, E. Golowich, B.R. Holstein and J. Trampetic, Phys. Rev. D 33, (1986) 179.

[6] T.E. Browder and S. Pakvasa, Phy. Lett. B 383 (1996) 475.

[7] Y. Nir and N. Seiberg, Phys. Lett. B 309 (1993) 337;
M. Leurer, Y. Nir and N. Seiberg, Nucl. Phys. B 420 (1994) 468.

[8] ALEPH Collaboration, *Improved measurements of electroweak parameters from Z decays into fermion pairs*, Z. Phys. C 53 (1992) 1.

[9] ALEPH Collaboration, *ALEPH: A detector for electron-positron annihilations at LEP*, Nucl. Instr. and Meth. A 294 (1990) 121.

[10] ALEPH Collaboration, *Performance of the ALEPH detector at LEP*, Nucl. Instr. and Meth. A 360 (1995) 481.

[11] ALEPH Collaboration, *Production of Charmed Mesons in Z Decays*, Z. Phys. C 62 (1994) 1.

[12] R.M. Barnett *et al.*, Phys. Rev. D 54 (1996) 1.

[13] T. Liu, *An Overview of* D^0–$\bar{D}^0$ *Mixing Search Techniques: Current Status and Future Prospects*, hep-ph/9508415, Presented at the τ-charm Factory Workshop, Argonne National Laboratory, June 20-23, 1995.

[14] ALEPH Collaboration, *A Measurement of* R_b *using Mutually Exclusive Tags*, Phys. Lett. B 401 (1997) 150.

[15] CLEO Collaboration, *Observation of* $D^0 \to K^+\pi^-$, Phys. Rev. Lett. 72 (1994) 1406.

[16] E691 Collaboration, *A Study of* D^0–$\bar{D}^0$ *Mixing*, Phys. Rev. Lett. 60 (1988) 1239.

[17] E791 Collaboration, *A Search for* D^0–$\bar{D}^0$ *Mixing and Doubly-Cabibbo-suppressed Decays of the* D^0 *in Hadronic Final States*, Phys. Rev. D 57 (1998) 13.

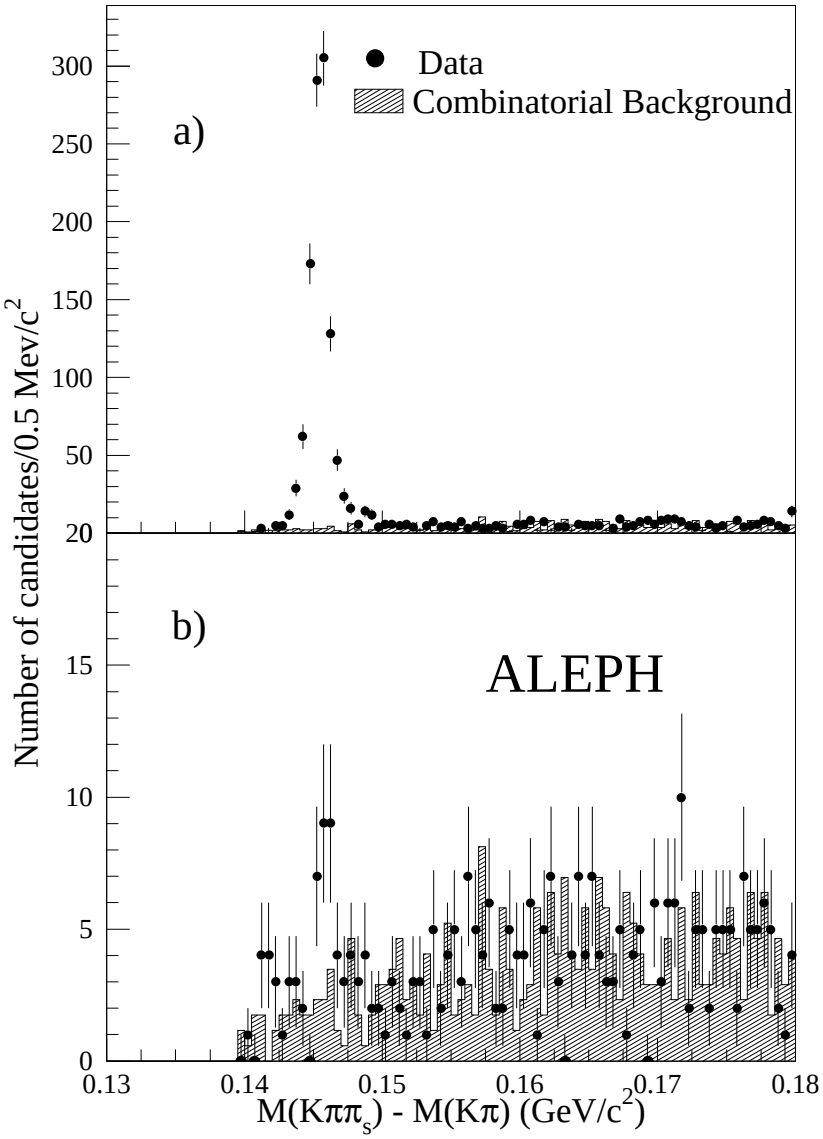

Figure 1: Mass-difference distribution (a) for candidates of the decay channel $D^{*+} \to D^0\pi_s^+$, $D^0 \to K^-\pi^+$ and (b) candidates of the decay channel $D^{*+} \to D^0\pi_s^+$, $D^0 \to K^+\pi^-$. The dots with error bars are data while the hatched histogram represents the distribution of the combinatorial background.

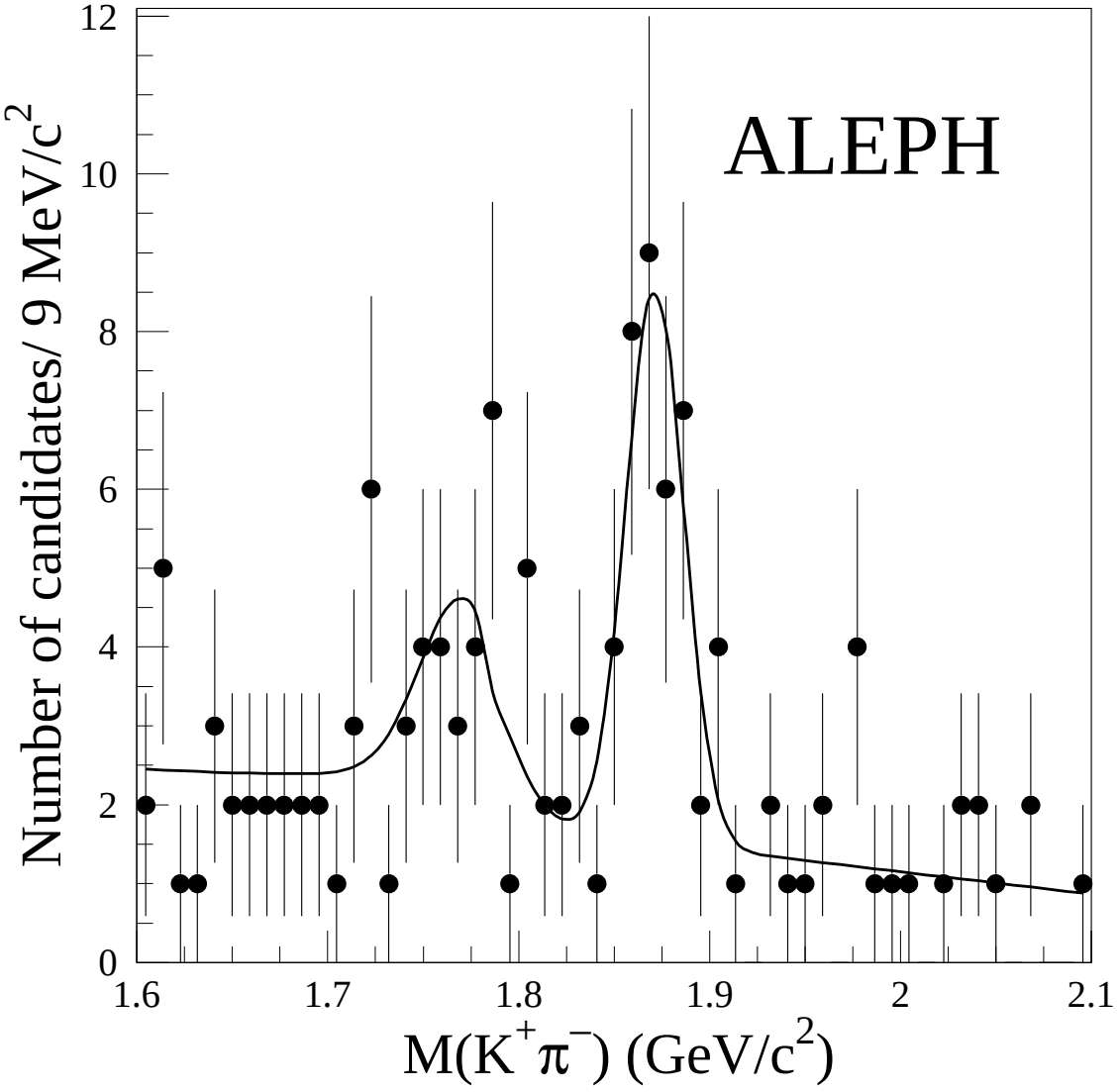

Figure 2: Mass distribution for candidates of the decay channel $D^{*+} \to D^0\pi_s^+$, $D^0 \to K^+\pi^-$. A narrow peak at the nominal D^0 mass ($M_{D^0} = 1864.5$ GeV/c^2) is present. The peak on the left is due to the decays $D^0 \to K^-K^+$ and is fitted taking the shape from Monte Carlo.

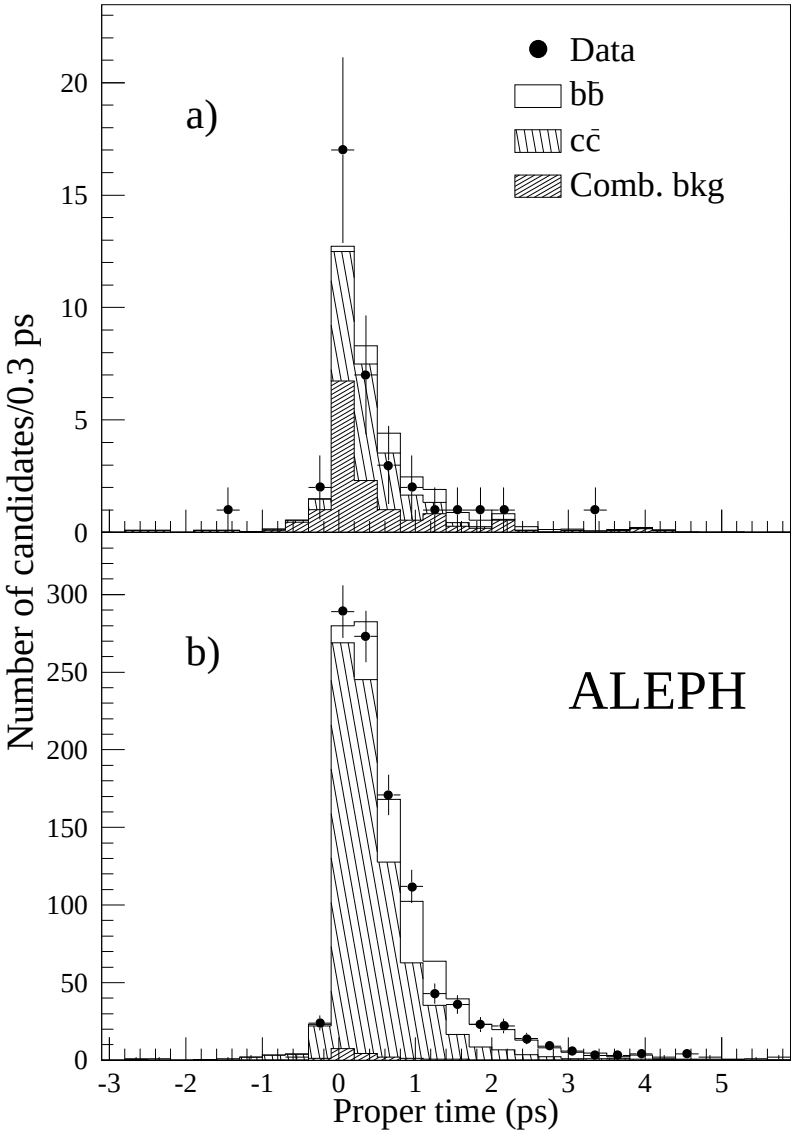

Figure 3: Proper time distribution for (a) the $D^0 \to K^+\pi^-$ candidates, and (b) for the $D^0 \to K^-\pi^+$ candidates. The dots with error bars are the data. The histograms are the contributions of $c\bar{c}$, $b\bar{b}$ and combinatorial background events resulting from the unconstrained fit when no interference is assumed.

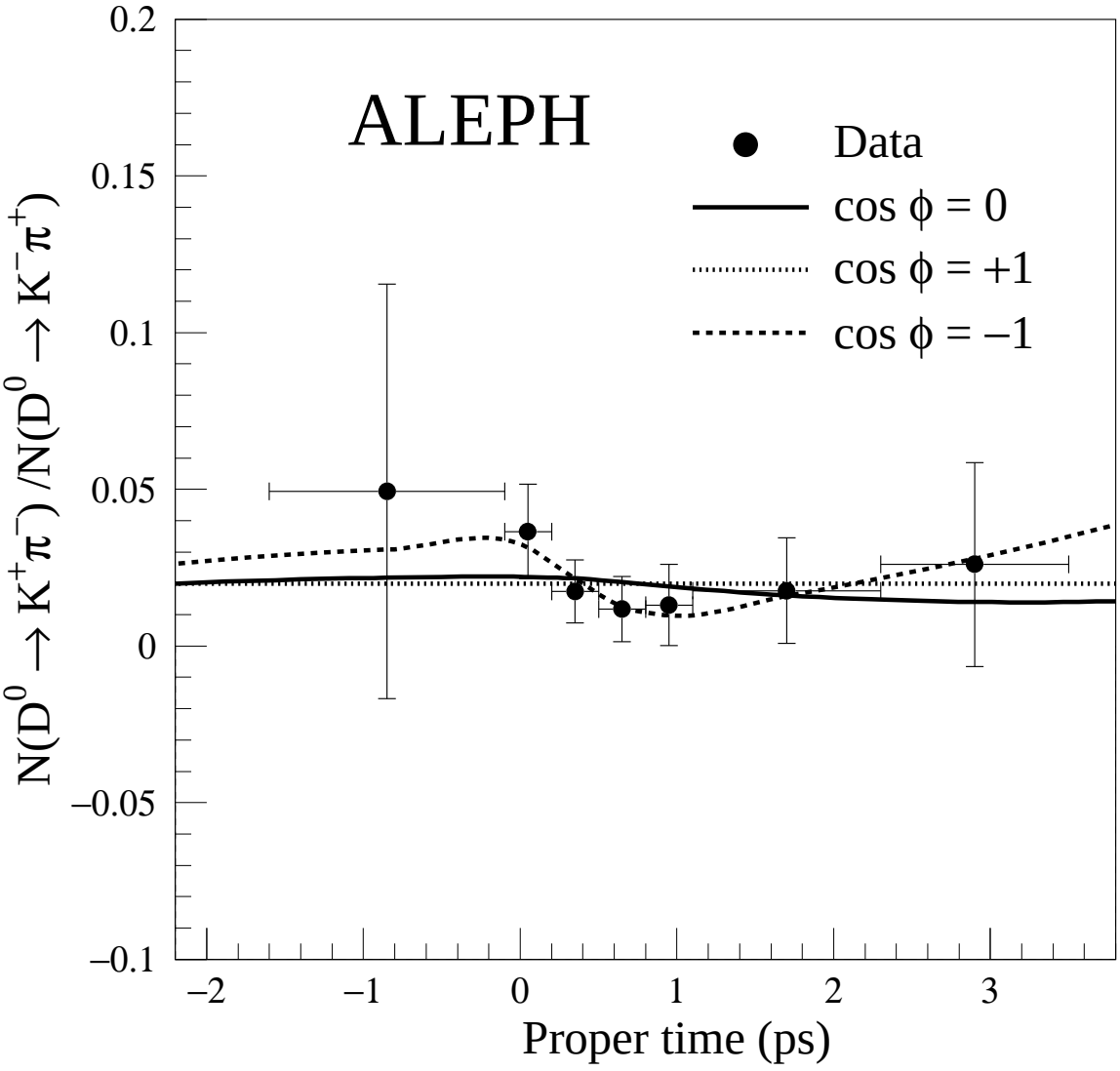

Figure 4: Proper time distribution of the $D^0 \to K^+\pi^-$ over $D^0 \to K^-\pi^+$ candidates with the background subtracted. The dots with error bars are data. The errors are the sum in quadrature of statistical and systematic uncertainties due to combinatorial background subtraction. The solid curve is the fit result with no interference, the dotted and dashed curves are the fit results assuming fully constructive and destructive interference, respectively.

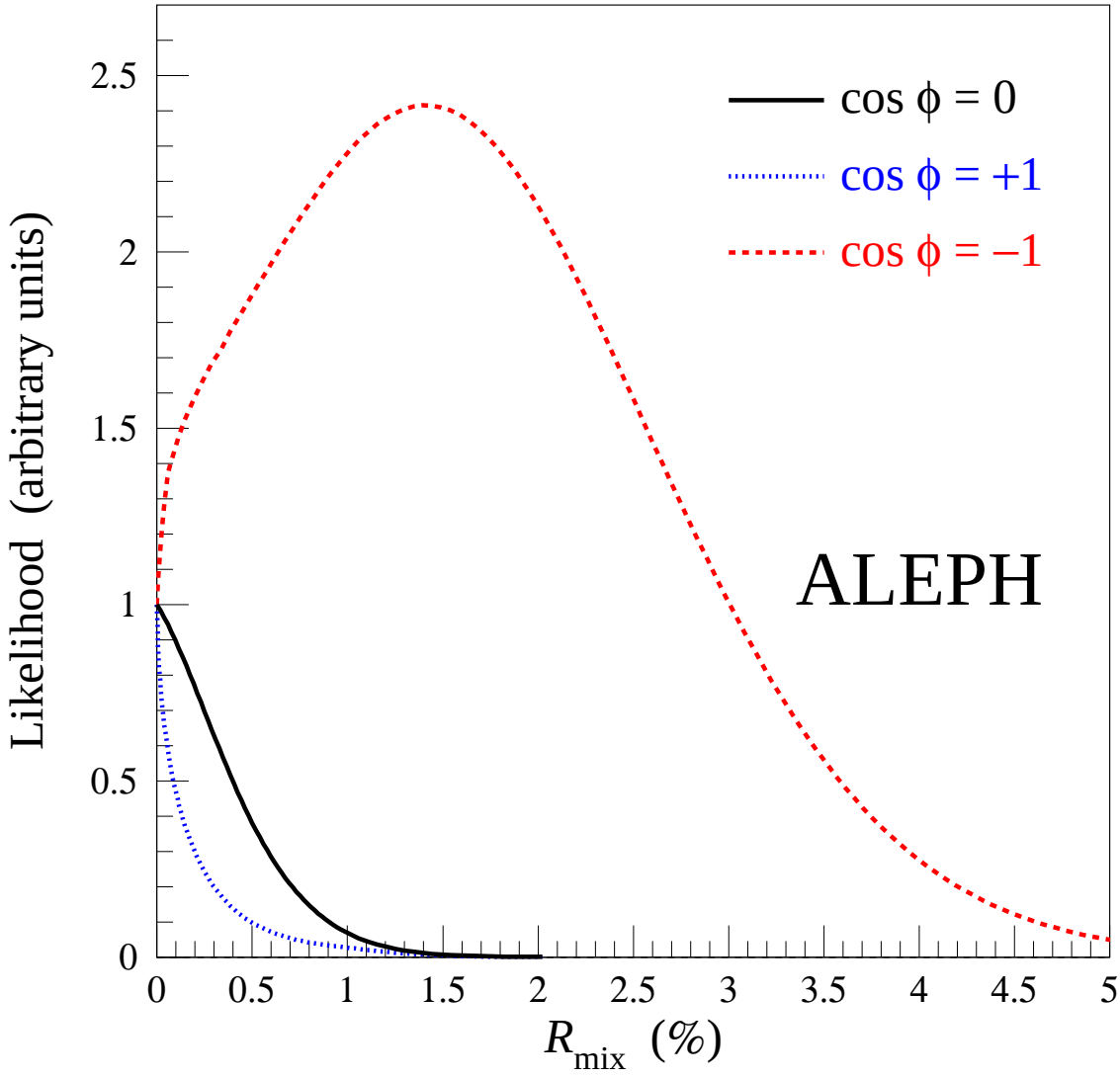

Figure 5: Likelihood of the fit as a function of R_{mix} calculated by leaving free the R_{DCSD} parameter and constraining all the external parameters within their uncertainties in order to take the systematic errors into account. The solid line represents the fit results with no interference, the dotted line is the likelihood for fully positive interference and the dashed line for fully negative interference.